International Core Journal of Engineering Volume 11 Issue 4, 2025
ISSN: 2414-1895 DOI: 10.6919/ICJE.202504_11(4).0051

Finite Element Analysis of the Influence of Texture Parameters on the Wear of Involute Spline Pairs

Xiangzhen Xue*, Zhaopeng Wu, Chen Wang, Ziang Bai, Ruming Ma, Haobo Zhang

Shaanxi University of Science and Technology, Mechanical and Electrical Engineering, Xi'an 710021, China

*Corresponding Author E-mail address: xuexiangzhen@sust.edu.cn (X. Xue).

Abstract

To design a PEEK based involute spline pair with better wear resistance, an orthogonal experimental scheme was designed. Based on the Archard wear model, the wear amount results under different texture parameter combinations were obtained using ABAQUS software.Establish a nonlinear regression model with the edge length, spacing, and depth of the texture as influencing factors, and wear amount as the output response index, to explore the influence of factors on the response index.Use range analysis to determine the primary and secondary order of influencing factors and use matrix analysis to determine the optimal parameter level of texture.The results indicate that:According to the wear simulation results under dry friction conditions, the presence of texture can effectively reduce the wear of spline tooth surfaces and improve their wear resistance;the primary and secondary order of the influence of texture edge length (*A*), spacing (*B*), and depth (*C*) on experimental indicators is *A*>*B*>*C*;the optimal parameter levels for texture are: edge length of 70um, spacing of 50um, and depth of 20um,this provides a theoretical basis for designing highly reliable, wear-resistant, and high-strength surface textured PEEK based involute spline pairs.

Keywords

Involute Spline; Archard Wear Model; Texture Parameters; Orthogonal Test; Nonlinear Regression Model.

1. Introduction

In mechanical transmission systems, involute splines are widely used as important connecting components in fields such as automobiles, aviation, ships, and heavy machinery. Their excellent load-bearing capacity and transmission efficiency make them one of the key components for connecting rotating parts[1]. However, as the operating time of the equipment increases, the wear problem of involute splines gradually becomes prominent, which not only affects the stability and efficiency of the transmission system, but may also lead to serious safety accidents. Due to its excellent wear resistance, lightweight, and good mechanical properties, PEEK based materials have been increasingly valued in recent years for their application and research in replacing transmission, braking, and other metal or aluminum components under light loads[2]. The use of PEEK based involute spline pairs instead of metal based involute spline pairs has been explored in certain fields for high-speed and light load applications[3]. The results showed that PEEK based aerospace involute spline pairs can effectively reduce the degree of wear on the surface of the spline pairs. In recent years, surface texturing technology has become a research hotspot for reducing interfacial friction and wear, and has been applied in multiple fields such as piston rings cylinder liners, mechanical seals, sliding bearings, molds, and cutting tools. Surface texturing is usually achieved by using

ISSN: 2414-1895 DOI: 10.6919/ICJE.202504_11(4).0051

chemical or physical methods to prepare micro/nanostructures on the surface of friction pairs to achieve non smooth surfaces[4-5]. Research has found that non smooth surfaces with regularly arranged morphologies/patterns exhibit excellent tribological properties[6-9]. At present, surface textures such as large pits, small pits, grooves, dents, ellipses, and circles at the micrometer or nanometer scale have been successfully applied to various material surfaces and achieved good wear reduction effects[10-12]. Therefore, scholars have attempted to apply tooth surface micro texturing technology combined with PEEK based materials to involute spline pairs. Given the crucial impact of tooth surface texturing parameters on the wear performance of textured components, studying the influence of different texturing parameters on the wear of involute splines is of great significance for the precise design of PEEK based aerospace involute spline pairs with tooth surface texturing.

2. Establishment of Finite Element Model for Involute Spline Pair

2.1 Geometric Model

The geometric model of the involute spline pair of PEEK based material is shown in Figure 1, where the internal spline is the active component and the external spline is the passive component. To meet the high-precision centering requirements, a large-diameter centering design is adopted, with a tooth flank clearance of 0.1167mm. The geometric parameters and material properties are detailed in Table 1.

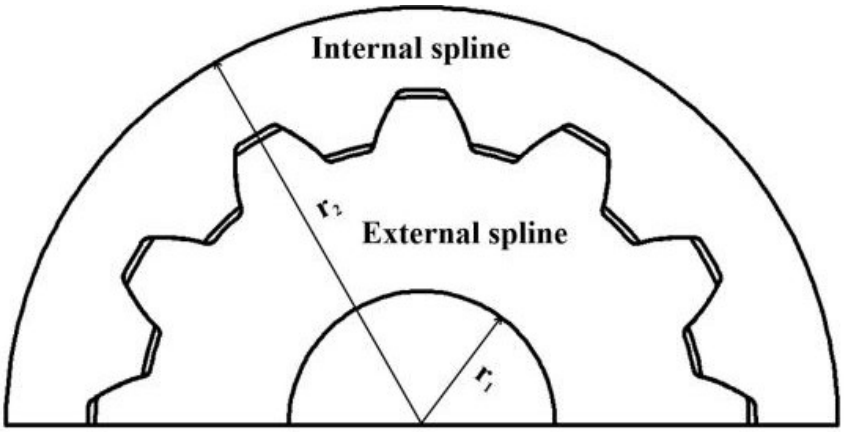

Figure 1. Geometric model of involute spline pair

Table 1. Parameters of involute spline pair

Parameter	Numerical value	Parameter	Numerical value
Number of teeth (Z)	12	Tooth width(D/mm)	9
Modulus(M/mm)	1.5	Bore diameter of external spline(r_1/mm)	10
Pressure angle(α/°)	30	Internal spline Journal(r_2/mm)	25

2.2 Establishment of Finite Element Model

A finite element model of the involute spline pair was established in Abaqus, as shown in Figure 2 (a). Using circumferential cyclic symmetry, analyze a pair of meshing key teeth as shown in Figure 2 (b). To save resources and ensure accuracy, as shown in Figure 2 (c), divide along the tooth width by 1/4 of the tooth width, refine the mesh in the meshing area, and roughen the remaining areas to improve efficiency, C3D8R elements are used. The model consists of 67228 units and 16802 nodes. A simplified model as shown in Figure 2 (c) was selected for simulation.

ISSN: 2414-1895 DOI: 10.6919/ICJE.202504_11(4).0051

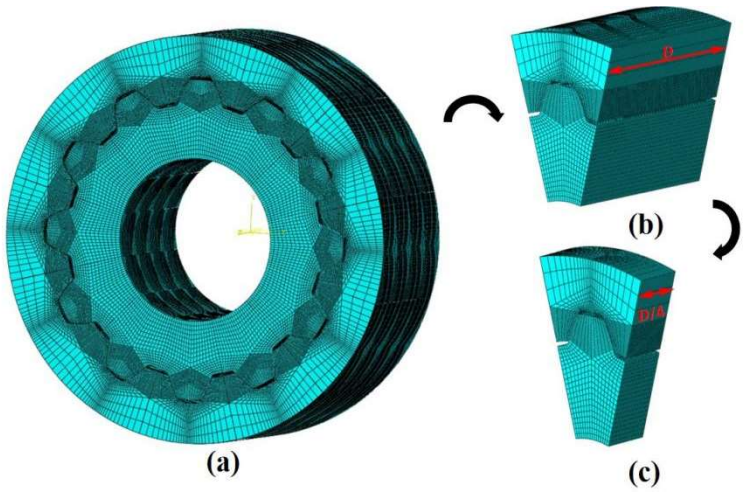

Figure 2. Finite element simulation model

2.3 Determination of Texture Position

The relevant research results indicate [13] that fractal structures can increase surface area, thereby exhibiting better performance in wear resistance and other aspects. In the field of tribology, fractal square texture can reduce friction coefficient and improve lubrication performance by increasing surface roughness. As shown in Figure 3, the fractal square texture of iteration 1 and iteration 2 is selected as the research object, with the meshing line of the internal and external splines as the axis of symmetry, placed on one side of the external spline tooth surface. For the convenience of expression, the fractal square texture iterated once is named Type I texture; The fractal square texture with 2 iterations is named type II texture.

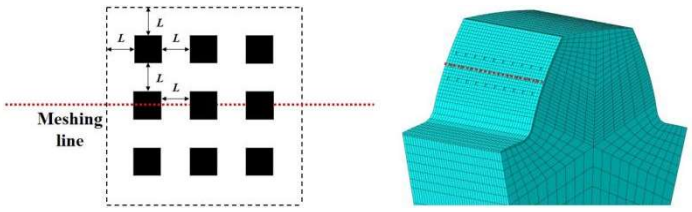

(a) Schematic diagram of type I pit texture

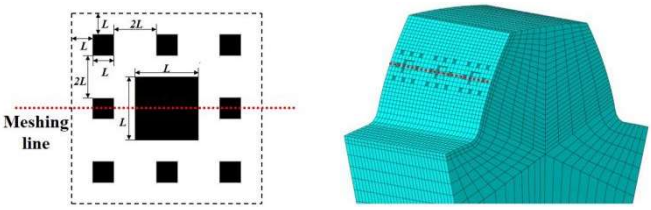

(b) Schematic diagram of type II pit texture

Figure 3. Texture distribution map

2.4 Finite Element Related Parameter Settings

The contact analysis of involute spline pairs is a nonlinear problem. The focus of this finite element calculation is on the wear of textured external spline teeth, so the mesh is refined and the internal spline mesh is not specially treated. The key tooth contact is set as surface to surface hard contact, with the internal spline as the main surface and the external spline as the secondary surface. Tangential behavior adopts a penalty function for hard contact, with a friction coefficient set to 0.3.

The boundary conditions are set as shown in Figure 4. The upper surface of the internal spline is coupled with RP1 point and subjected to torque, limiting its XYZ translational and XY rotational degrees of freedom, and only releasing Rz rotational degrees of freedom. The lower surface of the external spline is coupled by RP2 points and completely fixed. The torque size is 1/48 of the torque

ISSN: 2414-1895 DOI: 10.6919/ICJE.202504_11(4).0051

T transmitted by the spline pair, and periodic symmetrical boundaries are set on both sides of the dividing surface to ensure equivalent results. In this wear calculation section, the maximum incremental step size is 10000, the initial incremental step size is 0.01, the minimum incremental step size is 0.0001, and the maximum incremental step size is 0.2.

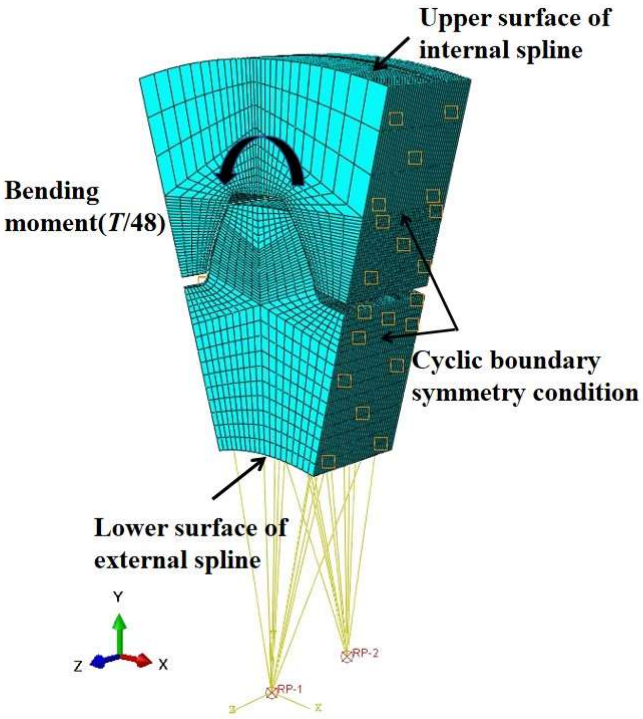

Figure 4. Boundary condition setting

2.5 Process for Estimating Wear of Involute Spline Pairs

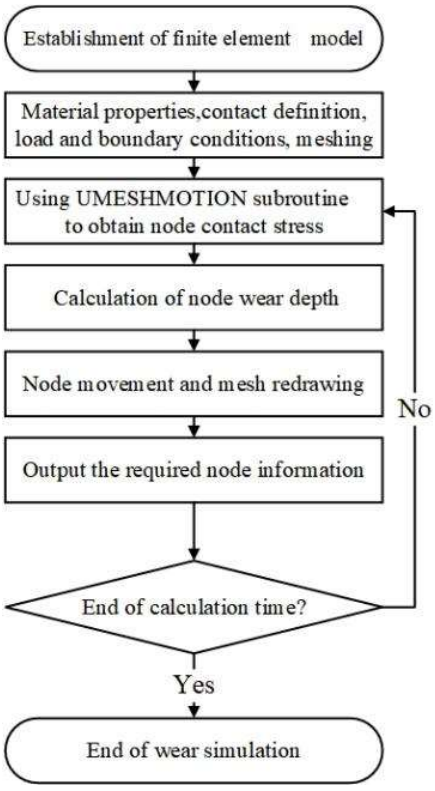

Figure 5. Wear simulation flowchart

ISSN: 2414-1895 DOI: 10.6919/ICJE.202504_11(4).0051

In ABAQUS, the UMESHMOTION subroutine is developed through secondary development, and the wear formula is written in Fortran language to achieve wear calculation. The wear direction is set as the normal direction of the contact surface. For corner nodes, they need to be renumbered to ensure correct wear direction. The UMESHMOTION subroutine calculates the wear depth at each incremental step and feeds back the results to ABAQUS. When calculating, the subroutine retrieves the node unit list and contact pressure information in order. The wear depth is represented by the node offset, which is determined based on the wear formula in the subroutine. To prevent grid distortion, ALE adaptive grid technology is adopted. Set the grid redraw frequency to 1 and the sweep frequency to 3 to optimize calculation accuracy and efficiency. The simulation process for wear of involute spline pairs is shown in Figure 5.

Finally, under normal temperature conditions, based on the Archard wear model simulation, the first set of simulation results in Table 3 for the wear depth of the external spline surface were obtained, as shown in Figure 6.

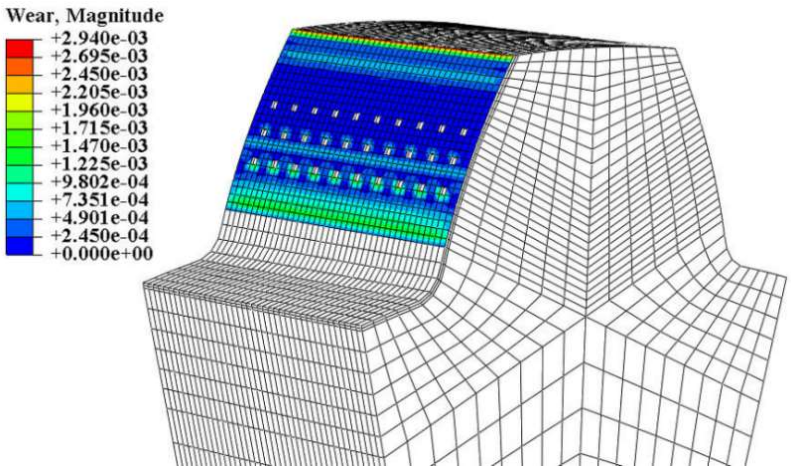

Figure 6. Abaqus simulation result chart

3. Orthogonal Design

3.1 Preliminary Determination of Surface Texture Shape

Design and study the Type I and Type II textures according to the organization parameters 1-6 in Table 3, and preliminarily select the texture shape with better wear performance for in-depth research. As shown in Figure 7, the finite element simulation results of the maximum wear depth of the tooth surface for two different texture shapes under the same texture parameter design are presented.

Obviously, with the simultaneous change of texture parameter groups, the trend of the change in wear depth of the two types of pit textures is almost consistent, showing a trend of first increasing and then decreasing; Overall, both textures demonstrate a certain degree of wear reduction effect. The simulated wear depth of type I pit texture under these 6 structural parameter groups is smaller than that of the involute spline of PEEK based material without texture; The simulated wear depth of Type II concave texture in the 1st, 2nd, 4th, 5th, and 6th structural parameter groups is smaller than that of the involute spline without texture, and only in the 3rd structural parameter group, the wear depth is greater than that of the involute spline without texture. Through these six sets of data, it can be found that the wear depth of type II pit texture shape is higher than that of type I pit texture shape under these six sets of texture parameters, and the average wear depth of each group is 1.4um higher. The reason for this situation may be that, under the same texture parameter group, the small square size in the middle of the Type II pit texture is too large, which reduces the contact area of the meshing area and increases the contact stress on the tooth surface, leading to increased wear on the spline tooth surface. Based on the above analysis, it has been preliminarily determined that Type I texture has better wear resistance performance, and further research will be conducted on this shape texture.

ISSN: 2414-1895 DOI: 10.6919/ICJE.202504_11(4).0051

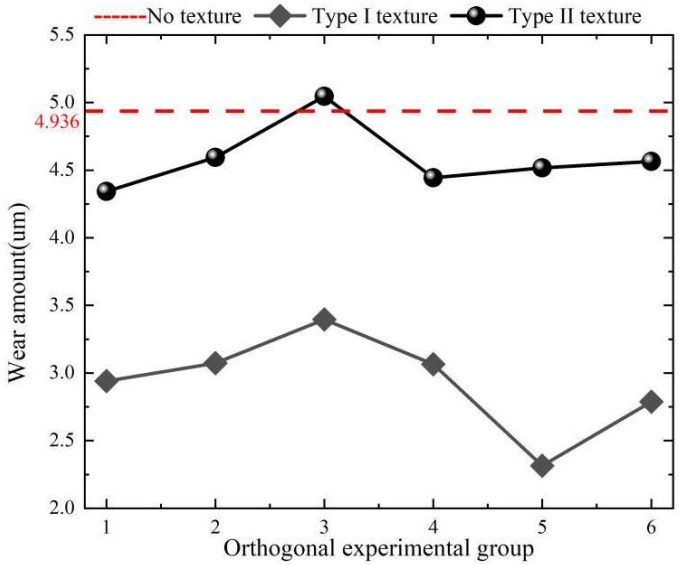

Figure 7. Comparison chart of wear depth under different texture shapes

3.2 Experimental Plan Design

Using finite element orthogonal experimental method, the influence of parameters such as edge length *A*, spacing *B*, and depth *C* of fractal square pit texture on wear amount was studied. Based on relevant literature [14] and the current achievable range of texture parameter processing, representative fractal square texture parameters and levels were designed, as shown in Table 2.

Table 2. Geometric parameters and levels of Type I texture

Level	Factor		
	Texture edge length(*A*)	Texture spacing(*B*)	Texture depth (*C*)
1	55	50	20
2	70	70	30
3	85	90	40
4	100	110	50

An experiment was designed using the L_{16} (3^4) orthogonal table for a surface pit texture with 3 factors and 4 levels for each factor. The specific experimental results are summarized in Table 3 for further analysis of the influence of various factors and their levels on texture properties, and based on this, the optimal design scheme is selected.

ISSN: 2414-1895 DOI: 10.6919/ICJE.202504_11(4).0051

Table 3. Corresponding relationship of wear amount under different texture parameters

Test number	Factor			Wear amount (um)
	A	*B*	*C*	
1	55	50	20	2.940
2	55	70	30	3.074
3	55	90	40	3.396
4	55	110	50	3.065
5	70	50	30	2.315
6	70	70	20	2.787
7	70	90	50	2.864
8	70	110	40	2.953
9	85	50	40	3.198
10	85	70	50	2.683
11	85	90	20	2.949
12	85	110	30	4.099
13	100	50	50	2.810
14	100	70	40	2.972
15	100	90	30	3.030
16	100	110	20	2.628
17	No texture			4.936
Ki1	12.475	11.263	11.304	
Ki2	10.919	11.516	12.518	
Ki3	12.929	12.239	12.519	
Ki4	11.44	12.745	11.422	
$\overline{\text{Ki1}}$	3.11875	2.81575	2.826	
$\overline{\text{Ki2}}$	2.72975	2.879	3.1295	
$\overline{\text{Ki3}}$	2.86	3.05975	3.12975	
$\overline{\text{Ki4}}$	3.23225	3.18625	2.8555	
R	0.5025	0.3705	0.30375	
Primary and secondary order	*A>B>C*			

Figure 8 shows a summary of 17 sets of experimental wear data in Table 3. Based on Table 3 and Figure 8, it can be seen that the wear amount of Type I texture under these 16 test numbers is lower than that of the spline of PEEK based material without texture. Among them, the results of the 5th, 10th, and 16th groups showed excellent wear resistance. The lowest wear amount in the 5th group was 2.315um, which was 53.1% less than that of the non textured spline. The results indicate that the

ISSN: 2414-1895 DOI: 10.6919/ICJE.202504_11(4).0051

presence of texture can effectively reduce the wear of the external spline tooth surface and improve the wear resistance of the spline to a certain extent.

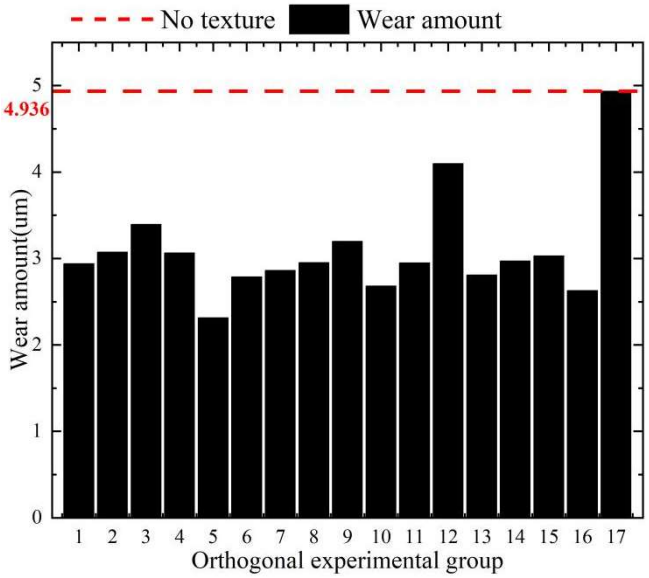

Figure 8. Summary of wear data under different texture parameters

According to the range analysis results in Table 3, the edge length of the pit (*A*) has the greatest impact on the wear amount (R=0.5025), while the depth of the pit (*C*) has the smallest impact on the wear amount (R=0.30375). The order of the influence of texture parameters on wear amount is: pit edge length (*A*)>pit spacing (*B*)>pit depth (*C*).

3.3 Analysis of Single Factor Simulation Results

3.3.1 Analysis of the Influence of Texture Edge Length on Wear Amount

Design a micro pit array on the external spline tooth surface and study the variation law of tooth surface wear depth when the texture edge length gradually increases from 55um to 100um. The analyzed bending moment is 50N · m. The finite element simulation results of the maximum wear depth of the tooth surface under different texture edge lengths are shown in Figure 9 (a). According to Figure 9 (a), it can be seen that under the premise of keeping other parameters of the texture unchanged, when the texture length is 70um, the maximum wear depth of the tooth surface is the smallest; When the texture length varies between 70-100um, the maximum wear depth of the tooth surface shows a gradually increasing trend, but overall it still exhibits a certain degree of wear reduction effect; When the texture edge length is 100um, the maximum wear depth of the tooth surface is the highest, with a value of 3.23225um.The results indicate that: Under dry friction conditions, the change in texture edge length has a significant impact on the wear depth of spline teeth. If the texture edge length is selected too large, it will cause pitting and wear on the tooth surface, so the texture edge length should not be selected too large.

3.3.2 Analysis of the Influence of Texture Spacing on Wear Amount

Design a pit array on the external spline tooth surface and study the changes in the maximum wear depth of the external spline tooth surface when the texture spacing is set to 50, 70, 90, and 110 μ m, respectively. The analyzed bending moment is 50N · m. The finite element simulation results of the maximum wear depth of the external spline tooth surface under different texture spacing are shown in Figure 9 (b). The results show that when the texture spacing is 50um, the maximum wear depth of the external spline tooth surface is the smallest, with a value of 2.81575um; As the texture spacing increases from 50um to 110um, the maximum wear depth of the external spline tooth surface

ISSN: 2414-1895 DOI: 10.6919/ICJE.202504_11(4).0051

increases with the increase of texture spacing; Overall, the larger the texture spacing, the greater the wear depth, and the poorer the wear reduction effect.

3.3.3 Analysis of the Influence of Texture Depth on Wear Amount

Design a pit array on the external spline tooth surface and study the changes in the maximum wear depth of the external spline tooth surface when the texture depth is taken as 20, 30, 40, and 50 μ m. The analyzed bending moment is 50 N · m. The finite element simulation results of the maximum wear depth of the tooth surface at different texture depths are shown in Figure 9 (c). It can be seen that, under the premise of keeping other parameters of the texture unchanged, as the depth of the texture increases, the maximum wear depth of the involute spline tooth surface of PEEK based materials shows a trend of first increasing and then gradually decreasing; When the texture depth is 30um and 40um, the maximum wear depth of the tooth surface of the external spline does not change much; When the texture depth is 20um, the external spline exhibits the best wear resistance.

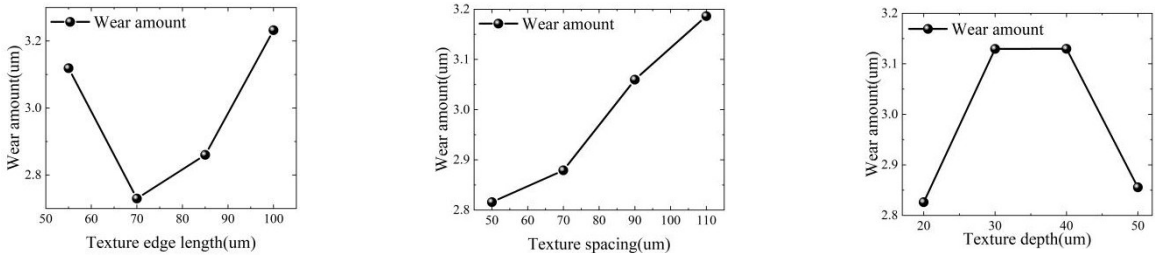

(a) Texture edge length (b) Texture spacing (c)Texture depth

Figure 9. The influence of various factors on wear and tear

4. Establishment of Multivariate Nonlinear Regression Equations

4.1 The Proposal of Multivariate Nonlinear Regression Equations

Orthogonal experimental design was used to obtain wear data under 16 organizational parameters. Analysis revealed that wear is influenced by complex interactions of multiple factors, and traditional methods are difficult to accurately describe. Therefore, multiple nonlinear analysis methods are introduced to construct accurate mathematical models based on their powerful modeling capabilities [15]. This study uses this method to predict wear, accurately capture changing trends, verify the accuracy of the model, and analyze relative errors to ensure the effectiveness and reliability of the model.

4.2 Determination of Single Factor Fitting Formula

The multiple nonlinear regression model is complex and difficult to implement directly in software. Therefore, this article adopts a step-by-step construction method: first, use univariate nonlinear regression to fit the formulas of various influencing factors and understand their nonlinear effects; Based on these formulas, multiple nonlinear formulas are synthesized through mathematical means to capture the interaction effects between factors; Finally, determine the statistical indicators to evaluate the fitting degree, stability, and predictive ability of the model. This method can effectively handle multiple nonlinear regression problems.

1) The equation for fitting the wear amount with respect to factor *A* is shown in equation (1), with a coefficient of determination R=0.976. The fitting curve result is shown in Figure 10 (a):

$$y_1=7.5844-0.128*x_1+0.000846*x_1^2 \quad (1)$$

2) The equation for fitting the wear amount with respect to factor *B* is shown in equation (2), with a coefficient of determination R2=0.983. The fitting curve result is shown in Figure 10 (b):

ISSN: 2414-1895 DOI: 10.6919/ICJE.202504_11(4).0051

$$y_2 = 2.701522 + 0.000136 * x_2 + 0.00004 * x_2^{\ 2} \quad (2)$$

3) The equation for fitting the wear amount with respect to factor *C* is shown in equation (3), with a coefficient of determination R2=0.999. The fitting curve result is shown in Figure 10 (c):

$$y_3 = 1.365312 + 0.101994 * x_3 - 0.001444 * x_3^{\ 2} \quad (3)$$

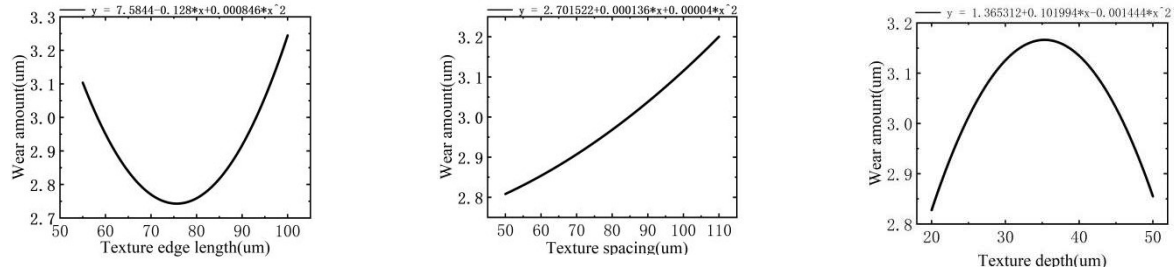

(a)Regarding *A* (b)Regarding *B* (c)Regarding *C*

Figure 10. Individual factor fitting curves

4.3 Fitting Multiple Nonlinear Regression Equations

Summarize the single factor fitting equation obtained in section 4.2 and obtain Table 4. According to the fitting equation of the relationship between wear depth and various factors in Table 4, a multiple regression model for wear depth was obtained through simple artificial synthesis [16], as shown in Equation (4):

Table 4. Summary of Single Factor Models

Factor	Equation	R2
A	$y_1=7.5844-0.128*x_1+0.000846*x_1^2$	0.976
B	$y_2 = 2.701522 + 0.000136 * x_2 + 0.00004 * x_2^{\ 2}$	0.983
C	$y_3 = 1.365312 + 0.101994 * x_3 - 0.001444 * x_3^{\ 2}$	0.999

$$y = a_1 + a_2 * y_1 + a_3 * y_2 + a_4 * y_3 \quad (4)$$

By substituting the fitted single factor equation, equation (5) is obtained:

$$y = b_{_1} + b_2 * x_1 + b_3 * x_1^2 + b_4 * x_2 + b_5 * x_2^2 + b_6 * x3 + b_7 * x_3^2 \quad (5)$$

In equation (5), y represents the maximum wear depth, um; x1 represents the texture edge length, um; x2 represents the texture spacing, um; x3 represents the texture depth, um. Based on the 16 sets of sample data in Table 3, select nonlinear regression in SPSS, input the regression model into the model expression, set initial values and constraints, and obtain a multivariate nonlinear regression equation about wear depth. In order to improve the goodness of fit and prediction accuracy of the regression model, a correction term is introduced on the basis of the original model, considering the interaction

ISSN: 2414-1895 DOI: 10.6919/ICJE.202504_11(4).0051

between various factors. The model expression after introducing the correction term [17] is shown in equation (6):

$$y = b_{1} + b_2 * x_1 + b_3 * x_1^2 + b_4 * x_2 + b_5 * x_2^2 + b_6 * x3 + b_7 * x_3^2 + \sum_{i=1,j=1}^{3} b_{ij} x_i x_j \quad (6)$$

The obtained multiple regression equation is shown in equation (7), with a coefficient of determination $R^2 = 0.902$.

$$\begin{aligned} y = {} & 1.1933 - 0.001 * x_1 + 0.000006 x_1^2 + 0.00065 * x_2 + 0.000185 * x_2^2 + 0.1037 * x_3 \\ & -0.0014 * x_3^2 - 0.00016 * x_1 x_2 + 0.00022 * x_1 x_3 + 0.0003 * x_2 x_3 \end{aligned} \quad (7)$$

4.4 Validation of Multivariate Nonlinear Regression Model

By comparing the orthogonal experimental data obtained through finite element analysis with the predicted data calculated by multiple linear regression model, the results are shown in Figure 11. From the graph, it can be seen that the predicted values obtained by the modified multivariate nonlinear mathematical model are consistent with the trend of the simulated values, and the two trends are basically the same. Only the error between the simulation data and the predicted data in Group 4 is greater than 10%. Although there are large errors in the predicted values, from the overall trend, the error between most predicted values and simulated values is effectively controlled within 10%. The average relative error between predicted data and simulated data is 3.76%. The results indicate that the constructed multiple linear regression model has good predictive accuracy and practicality, and can be used as an effective analytical tool for prediction and evaluation in related fields.

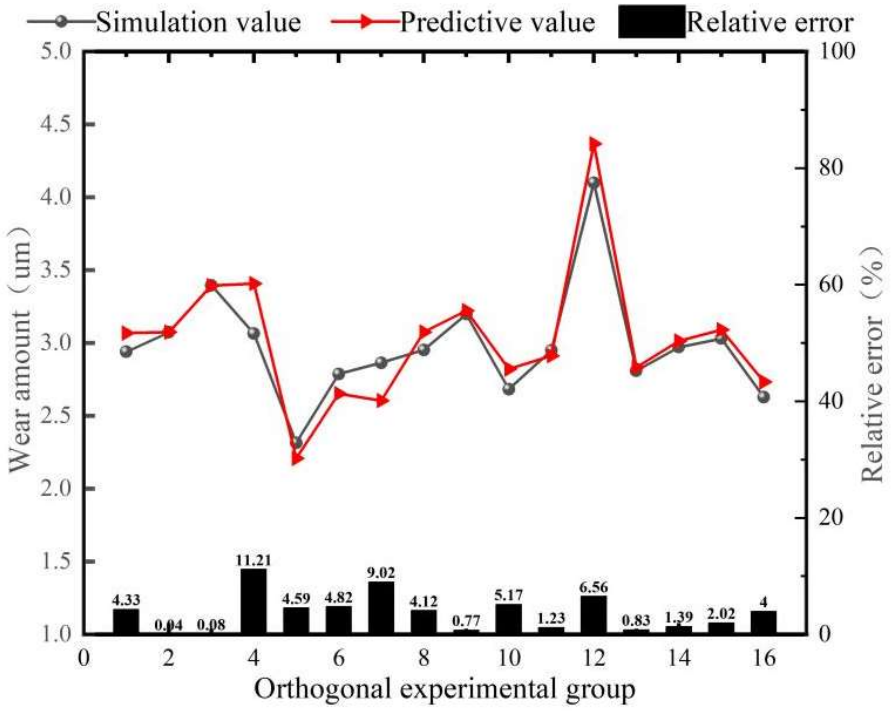

Figure 11. Comparison between wear prediction data and simulation data

ISSN: 2414-1895 DOI: 10.6919/ICJE.202504_11(4).0051

5. Surface Texture Optimization based on Orthogonal Experimental Design

The matrix analysis method deepens the processing of orthogonal experimental data by constructing a matrix to correlate performance indicators with factor levels, calculating influence weights, identifying optimal combinations, and ranking influencing factors. This method helps optimize experimental design and quickly locate key elements.

5.1 Constructing an Orthogonal Experimental Data Structure

Establish a data structure model based on the experimental data obtained from the orthogonal experimental scheme in Table 3. The structure model includes the experimental evaluation index layer, factor layer, and horizontal layer, as shown in Table 5.

Table 5. The data structure model of orthogonal experiment

Indicator layer	Inspection indicators		
Factor layer	Factor *A*	Factor *B*	Factor *C*
Horizontal layer	*A1*,*A2*,...,*An*	*B1*,*B2*,...,*Bn*	*C1*,*C2*,...,*Cn*

5.2 Construct Analysis Matrices at Various Levels

Based on the results of orthogonal experiments, this article establishes an evaluation and analysis matrix. In response to the different properties of indicators in optimization, define analysis matrices at each level, unify evaluation scales, and ensure comparability of weights.

5.2.1 Definition of Indicator Level Evaluation Matrix

The orthogonal experiment has m factors, each with n levels, and the arithmetic mean of the experimental index of factor *Ai* at the jth level is $\overline{k}_{ij}$. If it is required that the larger the experimental indicators, the better, then the indicator layer evaluation matrix $\boldsymbol{W}$ is defined as:

$$\boldsymbol{W} = \begin{bmatrix} \overline{k}_{11} & 0 & \cdots & 0 \\ \overline{k}_{12} & 0 & \cdots & 0 \\ \vdots & \vdots & \ddots & 0 \\ 0 & 0 & 0 & \overline{k}_{mn} \end{bmatrix} \tag{8}$$

If it is required that the smaller the experimental indicators, the better, then the indicator layer evaluation matrix $\boldsymbol{W}$ is defined as:

$$\boldsymbol{W} = \begin{bmatrix} \overline{k}_{11}^{-1} & 0 & \cdots & 0 \\ \overline{k}_{12}^{-1} & 0 & \cdots & 0 \\ \vdots & \vdots & \ddots & 0 \\ 0 & 0 & 0 & \overline{k}_{mn}^{-1} \end{bmatrix} \tag{9}$$

5.2.2 Definition of Factor Level Evaluation Matrix

If it is required that the larger the test index, the better, then let $e_i = 1/\sum_{j=1}^{n} \overline{k}_{ij}$; On the contrary, let $e_i = 1/\sum_{j=1}^{n} \overline{k}_{ij}^{-1}$. Where $e_i = 1/\sum_{j=1}^{n} \overline{k}_{ij}$ or $e_i = 1/\sum_{j=1}^{n} \overline{k}_{ij}^{-1}$ are the sum of the arithmetic mean values of I test indexes or their reciprocal obtained when the j-th parameter is taken at each level, then the factor layer evaluation matrix $\boldsymbol{E}$ is defined as:

ISSN: 2414-1895 DOI: 10.6919/ICJE.202504_11(4).0051

$$\boldsymbol{E} = \begin{bmatrix} e_1 & 0 & \cdots & 0 \\ 0 & e_2 & \cdots & 0 \\ \vdots & \vdots & \ddots & 0 \\ 0 & 0 & 0 & e_m \end{bmatrix} \tag{10}$$

5.2.3 Definition of Evaluation Matrix of Horizontal Layer

Let Ri be the range of the jth factor and let $t_i = R_i / \sum_{i=1}^{m} R_i$, then the evaluation matrix $\boldsymbol{T}$ of the horizontal layer is defined as:

$$\boldsymbol{T} = (t_1 \ t_2 \ \cdots \ t_m)^T \tag{11}$$

5.3 Constructing the Weight Matrix of Impact Assessment Indicators

The key of using matrix analysis method for optimization analysis is to determine the weight of evaluation index, which is related to the reliability of factor and level optimization results. The weight matrix $\boldsymbol{X}$ of impact assessment indicators is defined as:

$$\boldsymbol{X} = \boldsymbol{W} * \boldsymbol{E} * \boldsymbol{T} = (\omega_1 \ \omega_2 \ \cdots \ \omega_m)^T \tag{12}$$

Where, $\omega_1 = \overline{k}_{1j}^{\ -1} e_1 t_1$ represents the weight of the impact of the jth level of factor i on the evaluation index, which not only reflects the impact of the jth level of factor on the index, but also reflects the range of factors.

5.4 Weight Matrix Calculation of Wear Depth of Spline Tooth Surface of PEEK based Material

5.4.1 Wear Depth Evaluation Matrix *W*

In this study, the wear depth is taken as the test index. It is hoped that the smaller the wear depth of the spline tooth surface, the better. Then the wear depth evaluation matrix $\boldsymbol{W}$ is calculated according to formula (9):

$$\boldsymbol{W} = \begin{bmatrix} 0.3206 & 0 & 0 \\ 0.3663 & 0 & 0 \\ 0.3094 & 0 & 0 \\ 0.3497 & 0 & 0 \\ 0 & 0.3551 & 0 \\ 0 & 0.3473 & 0 \\ 0 & 0.3268 & 0 \\ 0 & 0.3138 & 0 \\ 0 & 0 & 0.3539 \\ 0 & 0 & 0.3195 \\ 0 & 0 & 0.3195 \\ 0 & 0 & 0.3502 \end{bmatrix}$$

5.4.2 Factor Level Evaluation Matrix *E*

In this study, the wear depth is taken as the test index. It is hoped that the smaller the wear depth of the spline tooth surface, the better. Then the wear evaluation matrix $\boldsymbol{E}$ is calculated according to formula (10):

ISSN: 2414-1895 DOI: 10.6919/ICJE.202504_11(4).0051

$$\boldsymbol{E} = \begin{bmatrix} \frac{1}{1.3460} & 0 & 0 \\ 0 & \frac{1}{1.3432} & 0 \\ 0 & 0 & \frac{1}{1.3431} \end{bmatrix}$$

$$= \begin{bmatrix} 0.7429 & 0 & 0 \\ 0 & 0.7445 & 0 \\ 0 & 0 & 0.7445 \end{bmatrix}$$

5.4.3 Horizontal Layer Evaluation Matrix $\boldsymbol{T}$

Calculate the horizontal layer evaluation matrix $\boldsymbol{T}$ according to formula (11):

$$\boldsymbol{T} = \begin{bmatrix} \frac{0.5052}{1.1768} \\ \frac{0.3705}{1.1768} \\ \frac{0.30375}{1.1768} \end{bmatrix}$$

$$= \begin{bmatrix} 0.4270 \\ 0.3149 \\ 0.2581 \end{bmatrix}$$

5.4.4Weight Matrix $\boldsymbol{X}$ Affecting Wear Depth

In this study, the wear amount is taken as the test index, and the weight matrix $\boldsymbol{X}$ affecting the wear amount of spline tooth surface is calculated according to formula (12):

$$\boldsymbol{X} = \boldsymbol{W} * \boldsymbol{E} * \boldsymbol{T} = \begin{bmatrix} 0.1017 \\ 0.1162 \\ 0.0981 \\ 0.1109 \\ 0.0833 \\ 0.0814 \\ 0.0766 \\ 0.0736 \\ 0.0680 \\ 0.0614 \\ 0.0614 \\ 0.0673 \end{bmatrix} = \begin{bmatrix} A1 \\ A2 \\ A3 \\ A4 \\ B1 \\ B2 \\ B3 \\ B4 \\ C1 \\ C2 \\ C3 \\ C4 \end{bmatrix}$$

The weight matrix $\boldsymbol{X}$ of the wear depth is calculated according to formula (12), where *A1-A4* are the weights of four levels corresponding to the side length of the pit texture on the involute spline tooth surface of PEEK based material respectively; *B1-B4* are the weights of the four levels corresponding to the tooth surface texture spacing, respectively; *C1-C4* are the weight of each level corresponding to the texture depth of tooth surface pits. From the calculation results, it can be concluded that among the four levels of factor *A*, *A2* has the largest weight; Among the four levels of factor *B*, *B1* has the largest weight; Among the four levels of factor *C*, *C1* has the largest weight. The greater the factor weight, the higher the impact on the results. Therefore, the optimal combination of texture parameters

ISSN: 2414-1895 DOI: 10.6919/ICJE.202504_11(4).0051

for wear resistance can be easily and quickly identified: *A*2*B*1*C*1, When the texture edge length is 70um, the texture spacing is 50um, and the texture depth is 20um, the wear resistance of the PEEK based material's spline tooth surface is optimal. When the wear resistance of the spline tooth surface is optimal, the weight value corresponding to *A2* (*A2*=0.1162) is the highest, followed by the weight value corresponding to *C1* (*C1*=0.0680), and the weight value corresponding to *B1* (*B1*=0.0833) is the lowest. The order of the influence of texture edge length (*A*), texture spacing (*B*), and texture depth (*C*) on experimental indicators is *A*>*B*>*C*.

6. Conclusion

(1) Under dry friction conditions, ABAQUS finite element wear simulation was conducted on the surface textured PEEK based involute spline. The results showed that the presence of texture can effectively reduce the wear of the external spline tooth surface and improve its wear resistance to a certain extent;

(2) The influence of texture parameters on the wear depth of PEEK based spline tooth surfaces was analyzed using range analysis method. The analysis results indicate that the primary and secondary order of the influence of texture parameters on wear depth is as follows: texture edge length (*A*)>texture spacing (*B*)>texture depth (*C*);

(3) The matrix analysis method based on orthogonal experimental design was used to study the influence of texture parameters on the spline wear performance of PEEK based materials. The optimal texture parameter combination *A*2*B*1*C*1 for wear performance was determined, that is, when the pit texture edge length is 70um, the pit texture spacing is 50um, and the pit texture depth is 20um, the wear resistance of the spline tooth surface is the best.

Acknowledgments

The author would like to express gratitude for the financial support provided by the National Science and Technology Major Project (Y2022-IV-0001-00180), Shaanxi Youth Innovation Team (2024), and Shaanxi Qinchuang Park "Scientists+Engineers" Team Construction (2024QCY-KXJ-112).

References

[1] Wang Yongliang, Zhao Guang, Sun Xucong, etc A review of research on aviation splines [J]. Aviation Manufacturing Technology, 2017, (03): 91-100.

[2] Wei Xiaojuan PEEK replaces metal materials in aircraft cabin door accessories [J]. Modern Plastic Processing Applications, 2016 (1): 37.

[3] Xue X, Yu W, Lin K, et al. Design Method and Teeth Contact Simulation of PEEK Involute Spline Couplings[J]. Materials, 2023, 17(1): 60.

[4] Han Y, Liu F, Zhang K, et al. A study on tribological properties of textured Co-Cr-Mo alloy for artificial hip joints[J]. International Journal of Refractory Metals and Hard Materials, 2021, 95: 105463.

[5] Zhang Q, Mei T, Zhang D, et al. Preparation of chemically etched surface texture and its friction characteristics in sheet forming[J]. Procedia Manufacturing, 2020, 50: 439-443.

[6] Tang Jie, Zeng Jie, Lu Xin The influence of T-shaped groove surface texture on the friction performance of metal rubber sealing pairs [J]. Machine Tool and Hydraulic, 2022, 50 (19): 134-139.

[7] Zhang N, Yang F, Jiang F, et al. Study of the effect of surface laser texture on tribological properties of cemented carbide materials[J]. Proceedings of the Institution of Mechanical Engineers, Part B: Journal of Engineering Manufacture, 2020, 234(6-7): 993-1006.

[8] Meng Y, Deng J, Zhang Y, et al. Tribological properties of textured surfaces fabricated on AISI 1045 steels by ultrasonic surface rolling under dry reciprocating sliding[J]. Wear, 2020, 460: 203488.

[9] Wang Z, Fu Q, Wood R J K, et al. Influence of bionic non-smooth surface texture on tribological characteristics of carbon-fiber-reinforced polyetheretherketone under seawater lubrication[J]. Tribology International, 2020, 144: 106100.

ISSN: 2414-1895 DOI: 10.6919/ICJE.202504_11(4).0051

[10] Zhan X, Yi P, Liu Y, et al. Effects of single-and multi-shape laser-textured surfaces on tribological properties under dry friction[J]. Proceedings of the Institution of Mechanical Engineers, Part C: Journal of Mechanical Engineering Science, 2020, 234(7): 1382-1392.

[11] Zhang Youjun, Sun Jingting, Yuan Zewei, etc The influence of surface microstructure on the wear resistance of joint bearings [J]. Journal of Shenyang University of Technology, 2021, 43 (02): 169-176.

[12] Paul Joshua S, Dinesh Babu P. Effect of laser textured surface with different patterns on tribological characteristics of bearing material AISI 52100[J]. Journal of Central South University, 2020, 27(8): 2210-2219.

[13] Wang Hongtao, Li Yan, Zhu Hua Research on the Lubrication and Friction Reduction Properties of Texture Surfaces with Fractal Features [J]. Surface Technology, 2016, 45 (09): 182-187.

[14] Renqing Duoji, Zhu Peiyuan, Chang Xuefeng, etc CFD analysis of lubrication performance of tooth groove texture considering cavitation effect [J]. Lubrication and Sealing, 2022, 47 (12): 91-99.

[15] Yang J, Chang J, Wang Y, et al. Comprehensive drought characteristics analysis based on a nonlinear multivariate drought index[J]. Journal of Hydrology, 2018, 557: 651-667.

[16] Cheng Maolin A method for establishing a multivariate nonlinear regression prediction model [J]. Statistical Education, 1997, (03): 23-24.

[17] Wu Jiali, Zhao Zhiman, Quan Sichen, etc Prediction of strength of phosphogypsum based on multiple nonlinear regression model [J]. Silicates Bulletin, 2017, 36 (11): 3770-3777.